Available online at www.sciencedirect.com

SciVerse ScienceDirect

journal homepage: www.elsevier.com/locate/he

In-situ measurement of ethanol tolerance in an operating fuel cell

Matt S. Naughton [a], *Claire E. Tornow* [b], *Yolanda Bonita* [a], *Huei-Ru "Molly" Jhong* [a], *Fikile R. Brushett* [a], *Andrew A. Gewirth* [b], *Paul J.A. Kenis* [a,*]

[a] *Department of Chemical & Biomolecular Engineering, University of Illinois at Urbana-Champaign, 600 S. Matthews Ave, Urbana, IL 61801, USA*

[b] *Department of Chemistry, University of Illinois at Urbana-Champaign, 600 S. Matthews Ave, Urbana, IL 61801, USA*

ARTICLE INFO

Article history:
Received 12 December 2012
Received in revised form
23 April 2013
Accepted 27 April 2013
Available online xxx

Keywords:
Alkaline fuel cell
Gas diffusion electrodes
Ag cathode
Electrode characterization
Reference electrode
Non-Platinum catalyst

ABSTRACT

Ethanol is seen as an attractive option as a fuel for direct ethanol fuel cells and as a source for on-demand production of hydrogen in portable applications. While the effect of ethanol on *in-situ* electrode behavior has been studied previously, these efforts have mostly been limited to qualitative analysis. In alkaline fuel cells, several cathode catalysts, including Pt, Cu triazole, and Ag can be used. Here, we apply a methodology using a microfluidic fuel cell to analyze *in-situ* the performance of these cathodes as well as Pt anodes in the presence of ethanol and acetic acid, a common side product from ethanol oxidation. For a given concentration of ethanol (or acetic acid), the best cathode catalyst can be determined and the kinetic losses due to the presence of ethanol (or acetic acid) can be quantified. These experiments also yield information about power density losses from the presence of contaminants such as ethanol or acetic acid in an alkaline fuel cell. The methodology demonstrated in these experiments will enable *in-situ* screening of new cathodes with respect to contaminant tolerance and determining optimal operational conditions for alkaline ethanol fuel cells.

1. Introduction

Direct ethanol fuel cells are emerging as promising power sources due to the availability of bioethanol [1,2]. Ethanol is a liquid at ambient conditions, is relatively non-toxic, and has a high theoretical energy density of 8.0 kWh/kg [3,4]. Furthermore, fuel cells are inherently more efficient than, for example, combustion-based power generation processes [5]. The use of carbon-based fuels in alkaline fuel cells has historically been limited by carbonate formation from CO_2, which has prevented long-term operation in alkaline media [5–7]. More recently, alkaline membrane-based fuel cells have emerged to counteract the problem of carbonate formation [1,4,8,9]. Full electro-oxidation of ethanol still remains a challenge.

In a fuel cell, ethanol can fully oxidize to carbon dioxide, producing 12 electrons, or partially oxidize to acetaldehyde or acetic acid, producing two or four electrons respectively along with water [4,10]. Common ethanol oxidation catalysts are based on Pt in acidic or alkaline media or Pd in alkaline media, but novel catalysts based on other metals are still being developed [11–14]. The commonly used PtRu and PtSn anode

* *Corresponding author*. Tel.: +1 217 265 0523; fax: +1 217 333 5052.
E-mail address: kenis@illinois.edu (P.J.A. Kenis).

0360-3199/$ – see front matter
http://dx.doi.org/10.1016/j.ijhydene.2013.04.147

catalysts are relatively unselective for full oxidation, producing less than 11% CO_2 [4,15]. For example, an alkaline fuel cell with a PtSn anode was >90% selective for the formation of acetic acid when operated at a current density of 20 mA/cm^2, while the same configuration operated at 60 mA/cm^2 produced acetic acid as well as acetaldehyde in significant amounts [4]. Thus, analysis of ethanol tolerance should also include an analysis of acetic acid tolerance.

While much research has focused on improved *anode* catalysis for ethanol fuel cells, ethanol-tolerant *cathode* catalysts are also a key to maximizing direct ethanol fuel cell performance and efficiency [11]. Ethanol crossover from the anode can cause mixed potentials at the cathode, reducing cathode performance and fuel utilization. This problem is aggravated with higher ethanol concentrations, even though those concentrations may be necessary for better anode kinetics. As a result, cathode catalysts that exhibit selectivity towards the oxygen reduction reaction (ORR) and are unaffected by the presence of ethanol or its degradation products are essential for high-performance direct ethanol fuel cells.

Prior work to analyze cathode performance in the presence of ethanol has largely been limited to *ex-situ* rotating disk electrode (RDE) experiments, which do not accurately replicate fuel cell operating conditions [16]. For example, work by Jiang et al. showed that the onset potential for Pt/C in O_2-saturated 0.1 M NaOH dropped by approximately 0.07 V in the presence of 0.05 M EtOH [17]. While this result illustrates the sensitivity of Pt to ethanol poisoning, the solubility of O_2 in pure water is only 1.25 mM, which is far lower than the 40 mM supply from convected O_2 or the 8 mM supply of O_2 from convected air, and indicates an unfavorable ethanol to O_2 molar ratio of 40 [18]. Additionally, an alkaline membrane or liquid fuel cell would typically contain a hydroxyl concentration of 1 M or greater (pH $\geq$ 14), instead of the pH 13 found in these RDE experiments. While membrane-based systems intrinsically operate under fuel cell conditions, precise manipulation of the electrolyte is considerably more difficult than it is in liquid electrolyte-based systems, and the lack of a reference electrode in a membrane-based system hampers differentiation between anode and cathode effects.

Similarly, ethanol tolerance of electrodes is also important for hydrogen fuel cells that receive their H_2 feed from the reforming of ethanol. Ethanol is a means to store hydrogen in the liquid phase, but contamination of the hydrogen fuel feed with ethanol and byproducts such as acetic acid have prevented system implementation to date [19–22]. In addition, the loss in performance due to ethanol and acetic acid contamination within an operating H_2 fuel cell has not been quantified.

Here, we use a microfluidic hydrogen-oxygen (H_2/O_2) fuel cell with a flowing alkaline electrolyte stream [23–25] to characterize and quantify the effect of ethanol contaminant on Pt [4], Ag [7], and Cu triazole [26] electrodes. Although these catalysts have been tested in various fuel cell setups, they have not been compared to each other in the presence of ethanol. Determination of cathode performance *in-situ*, in an actual fuel cell, is a more accurate means to determine relative performance and discover which catalyst performs better under realistic operating conditions. The use of a hydrogen fuel cell here, instead of a direct ethanol fuel cell, allows us to achieve higher current densities at the cathode while at the same time we can control the amount of ethanol, as a contaminant, in the cell. Here we use a microfluidic fuel cell with a reference electrode [27] in combination with an analytical method that we developed previously [28] to quantify single electrode behavior within an operating fuel cell, specifically the effects of ethanol and acetic acid contamination on cathodes and anodes. Using this method, we determine whether the expensive Pt catalyst or the non-noble metal alternative Ag is superior for a given ethanol contaminations and we demonstrate the ability to screen new cathode catalysts by quantifying the effect of ethanol on Cu triazole. We also discuss the importance of the ethanol to oxygen molar ratio when determining ethanol tolerance.

2. Experimental section

2.1. Gas diffusion electrode preparation

For Pt and Ag, commercially available Pt/C (50% mass on Vulcan carbon, E-Tek) or Ag/C (60% mass on Vulcan carbon, E-Tek) were used as electrode catalysts. For Cu triazole, the catalyst was prepared using the procedure developed by Thorum et al., except that centrifugation was used instead of suction filtration [29]. In brief, $CuSO_4$ (Aldrich) was sonicated with Vulcan XC-72 in water; a solution of 3,5-diamino-1,2,4-triazole (Aldrich) was then added dropwise and the solution was again sonicated. The catalyst was centrifuged to remove the supernatant and dried under vacuum at 90 °C [29]. The copper loading of the Cu triazole/C was determined by elemental analysis using an ELAN DRCe ICP-MS (Dynamic Reaction Cell Inductively Coupled Plasma-Mass Spectrometer) (Perkin Elmer SCIEX) to be 2.84 wt%, which is lower than the previously used Cu loading of 3.76 wt%. The N:Cu ratio was 4.91:1, which matches the N:Cu ratio of 5:1 calculated from the crystal structure. A 30:1 ratio of catalyst to Nafion was used as the catalyst binder such that catalyst inks were prepared by mixing a total of 8.0 mg of Pt/C or 27 mg of Ag/C and 6.13 μL or 20.4 μL of 5 wt% Nafion solution (DuPont), respectively [24,26]. 200 μL of DI water and 200 μL of isopropyl alcohol (Fisher Scientific) were added as carrier solvents. The catalyst inks were sonicated (Branson 3510) for 1 h to obtain a uniform mixture, which was then hand-painted onto 4 cm^2 of the hydrophobized carbon side of a carbon paper gas diffusion layer (35 BC, SGL carbon group) to create a gas diffusion electrode (GDE). The final catalyst loading was 1 mg/cm^2 of Pt (50% mass Pt) for the anode and 1 mg/cm^2 of Pt (50% mass Pt), 4 mg/cm^2 of Ag (60% mass Ag), or 4 mg/cm^2 of Cu triazole/C for the cathode.

2.2. Fuel cell assembly and testing

To assemble the fuel cell, shown in Fig. 1, the cathode (Pt/C or Ag/C) and the anode (Pt/C) were placed on the opposite sides of a 0.1-cm or 0.2-cm thick polymethylmethacrylate (PMMA) window, such that the catalyst-coated GDE sides face the 3-cm long and 0.33-cm wide window machined in PMMA [24]. The microfluidic chamber volume was 0.2 ml. The window has one inlet and one outlet from the side for the electrolyte flow, aqueous solutions of potassium hydroxide (KOH,

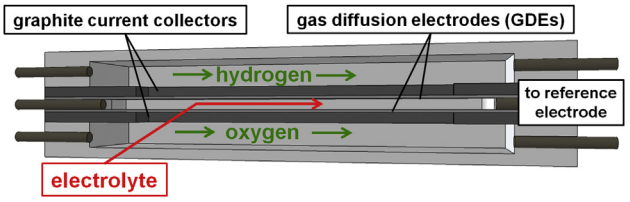

Fig. 1 – Diagram of a microfluidic fuel cell with a flowing alkaline electrolyte.

Sigma–Aldrich, 85%, balance of H_2O) or sulfuric acid (H_2SO_4, Mallinckrodt, 95–98%, balance of H_2O). Two 1-mm thick graphite windows were used as current collectors. Polycarbonate gas flow chambers (5 cm (L) × 1 cm (W) × 0.5 cm (H)) were used to introduce both hydrogen and oxygen gases (laboratory grade, S.J. Smith), at 10 sccm each. In both cases, the multilayer assemblies were held together with binder clips (Highmark). Fuel cell testing was conducted using a potentiostat (Autolab PGSTA-30, EcoChemie) at room temperature. For all studies, electrolyte flow rate was maintained at 0.3 mL min^{-1} using a syringe pump (2000 PHD, Harvard Apparatus) [23]. Prior to experiments using the Ag cathode, the fuel cell was operated at 0.3 V for 20 min to activate the catalyst [30]. Fuel cell polarization curves were obtained by measuring steady-state currents at different cell potentials using General Purpose Electrochemical System (GPES) software (EcoChemie). The exposed geometric surface area of the electrode (1 cm^2) was used to calculate the current and power densities. A reference electrode (Ag/AgCl in saturated NaCl, BASi) was placed at the outlet of the electrolyte stream to allow for the independent analysis of polarization losses on the cathode and the anode [27]. The reference electrode was fitted with a polyethylene frit (Princeton Applied Research) in place of the original Vycor® frit to prevent corrosion and contamination in alkaline media. After each experiment, the fuel cell was disassembled and the electrodes were rinsed with deionized water, then dried under a laboratory fume hood.

2.3. *Rotating ring-disk electrode (RRDE)*

A catalyst ink containing Pt/C (1.0 mg mL^{-1}) (20% mass on Vulcan carbon, E-Tek) was prepared with Nafion solution (4 μL mL^{-1} 5%, Aldrich) in water and briefly sonicated. A 20-μL drop was deposited onto a polished (0.05 μ alumina) glassy carbon disk (0.196 cm^2) with a Pt ring (Pine Instruments) and dried under a stream of Ar. Electrochemical measurements were collected using a CHI 760D bipotentiostat (CH Instruments) using a Pt gauze counter electrode and a "no-leak" Ag/AgCl reference electrode (Cypress Systems), separated from the RRDE by a Luggin capillary. The reference electrode was calibrated to the RHE scale by saturating the cell with H_2 and measuring the open circuit potential at the Pt ring electrode.

2.4. *Conductivity measurements*

The room temperature conductivity of electrolyte solutions was measured with an pH/conductivity meter (Thermo Scientific - Orion 4 star) using a two-electrode conductivity cell (Duraprobe 018020MD). Before measurement, the conductivity cell was triple rinsed with deionized water and calibrated with a 1 M KCl solution with a conductivity of 111.9 mS cm^{-1}.

3. Results and discussion

Several catalysts that have shown promise for oxygen reduction in alkaline media are tested here. *Platinum* is known to have high activity in alkaline media and is typically used as a performance standard [7,31]. However, platinum also catalyzes the oxidation of fuels such as ethanol and other alcohols, and as a result non-Pt catalysts that are more selective toward oxygen reduction have gained increasing attention [1,12,32]. *Silver* is stable in alkaline media, much cheaper than platinum, and unlike platinum it does not catalyze ethanol oxidation [12,31]. The disadvantage of silver relative to platinum is its lower catalytic activity [7,23,31]. Recently, we reported on *Cu*

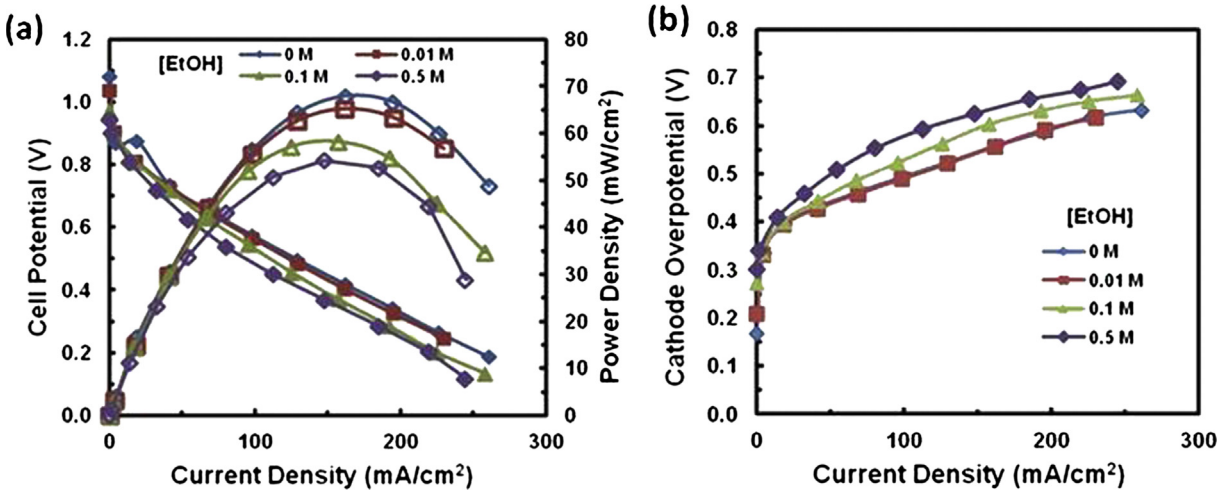

Fig. 2 – (a) Power density and polarization curves and (b) cathode overpotential curves as a function of current density for varying ethanol concentrations when using a Pt cathode. Anode: Pt/C (1 mg Pt/cm^2); cathode: Pt/C (1 mg Pt/cm^2); electrolyte: 1 M KOH; electrolyte flow rate: 0.6 ml/min; H_2/O_2 feeds: 10 SCCM. At room temperature.

Table 1 – Quantitative fits for Pt cathode with varying [EtOH].

[EtOH] (M)	cathode $\eta_{kinetic}$ (V)	cathode R_{ohmic} (Ω–cm^2)	Anode $\eta_{kinetic}$ (V)	Anode R_{ohmic} (Ω–cm^2)
0	0.39	1.01	0.01	1.54
0.01	0.39	1.03	0.02	1.62
0.1	0.40	1.33	0.01	1.62
0.5	0.45	1.25	0.02	1.49

triazole, a biomimetic catalyst, which is highly selective for the ORR [26,29,33]. Cu triazole outperformed silver on a mass activity basis in an alkaline fuel cell. These catalysts have been studied in more detail elsewhere for Pt [16,23,34], Ag [23,26], and Cu triazole [26,29,33]. The method used here focuses on individual electrode plots, which are obtained by tracking the electrode potentials of each electrode during fuel cell operation [28]. Thus, the data here is for electrodes under fuel cell operating conditions, but is specific to each electrode as a function of current density without being a direct function of fuel cell load. Here, we examine each of these catalysts as a function of ethanol concentration using this analytical method.

3.1. *Effect of ethanol on a Pt cathode*

The effect of ethanol on a Pt cathode was tested using the microfluidic fuel cell (Fig. 1), equipped with a Pt anode as the counter electrode, and operated with hydrogen and oxygen reactant feeds. An aqueous 1 M KOH electrolyte with varying concentrations of ethanol (0, 0.01, 0.1, and 0.5 M) was continually flowed into the cell between the anode and the cathode. The polarization and power density curves exhibit a steady drop in power density with increasing ethanol concentration (Fig. 2). To further analyze the effects of the ethanol contamination on the cathode, we used single electrode plots based on overpotential as we described previously [28]. A linear fit applied to the ohmic region of these single electrode plots yields R_{ohmic}, a parameter that contains contributions from kinetic, ohmic, and mass transport effects, as well as $\eta_{kinetic}$, a parameter that contains contributions from kinetic and crossover losses [28]. The lack of change in cathode performance up to ethanol concentrations of 0.01 M (Fig. 2b) indicates that the Pt cathode is tolerant up to that point. While the cathode exposed to 0.01 M EtOH has a higher overpotential at zero current, this decrease does not result in inferior performance under load. However, a greater overpotential when the electrode is exposed to 0.1 M EtOH clearly indicates a decrease in performance in broad agreement with the voltage loss shown by Jiang et al. [17]. Specifically, R_{ohmic} increases by 31% (Table 1). This type of increase in R_{ohmic} but almost no change in $\eta_{kinetic}$ (Table 1) is typically correlated with decreased catalyst utilization or decreased reactant transport [28]. In this case, ethanol or its degradation products may be blocking catalytic sites or blocking the transport of oxygen to those catalytic sites. The constant $\eta_{kinetic}$ may indicate that ethanol is not reacting in significant quantities at the electrode.

The performance of the cathode further degrades in the presence of 0.5 M EtOH, showing a 0.05 V decrease in $\eta_{kinetic}$. The corresponding decrease in maximum power density, assuming no loss in anode performance, is expected to be equal to the change in $\eta_{kinetic}$ divided by the potential used to obtain maximum power density. In this case, a 14% decrease in the maximum power density would be predicted, assuming maximum power was obtained at 0.4 V. The actual measured decrease in maximum power density is 20%, caused by a 23% increase in R_{ohmic} compared to the initial performance in the absence of ethanol. This voltage loss of 0.05 is similar to the

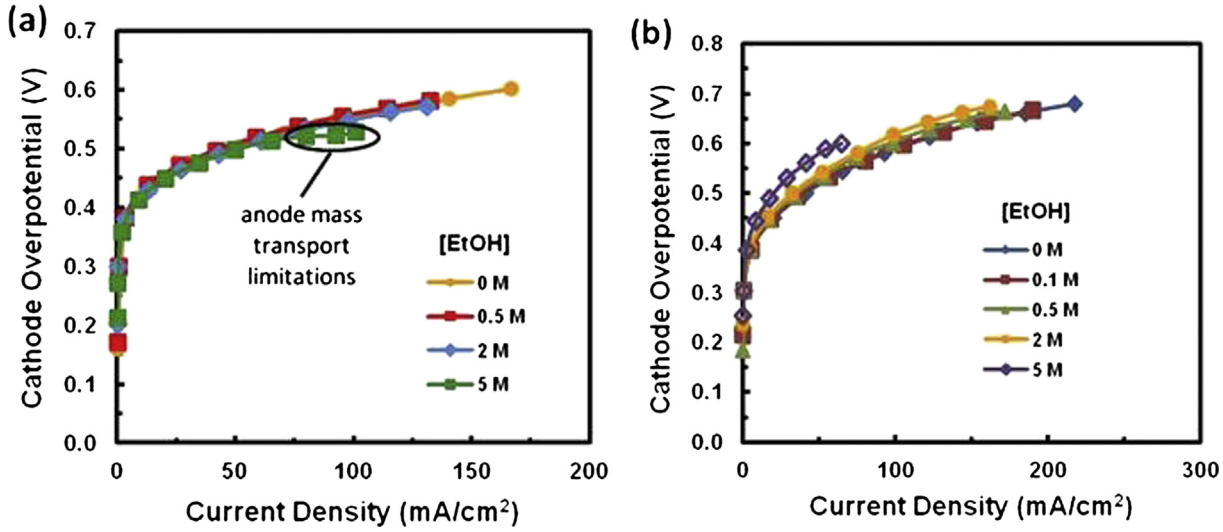

Fig. 3 – Cathode overpotential curve for varying ethanol concentrations as a function of current density for (a) a 4 mg/cm^2 Ag cathode or (b) a 4 mg/cm^2 Cu triazole cathode. Anode: Pt/C (1 mg Pt/cm^2); electrolyte: 1 M KOH; electrolyte flow rate: 0.6 ml/min; H_2/O_2 feeds: 10 SCCM. At room temperature.

Table 2 – Quantitative fits for Cu triazole cathode with varying [EtOH].

[EtOH] (M)	Cathode $\eta_{kinetic}$ (V)	Cathode R_{ohmic} (Ω–cm^2)	Anode $\eta_{kinetic}$ (V)	Anode R_{ohmic} (Ω–cm^2)
0	0.47	1.21	0.03	1.69
0.1	0.47	1.20	0.04	1.77
0.5	0.47	1.32	0.03	1.95
1	0.49	1.40	0.02	2.08
5	0.44	2.99	0.05	4.62

0.07 V loss observed in the RDE system of Jiang et al. [17]. Although the absolute amount of ethanol in that system is only 0.05 M EtOH, our system operating with 0.5 M EtOH and pure oxygen actually has a smaller ethanol to oxygen molar ratio of 12.5 as compared to the RDE ethanol to oxygen molar ratio of 40. The relative amounts of contaminant and oxidant, here oxygen, in the system play a key role in determining the electrode tolerance. These results demonstrate that ethanol crossover substantially affects Pt cathode performance, necessitating a barrier between the ethanol feed and the cathode if a Pt cathode is used.

3.2. *Effect of ethanol on a Ag cathode*

Ag is a common cathode catalyst in alkaline media and, as a non Pt-group metal, is less likely to be affected by the presence of ethanol. To determine the effect of ethanol on Ag electrode performance, the microfluidic fuel cell was operated as before using 1 M KOH electrolyte with ethanol concentrations up to 5 M. Fig. 3a shows that the Ag cathode is insensitive to ethanol at concentrations up to 5 M $\eta_{kinetic}$ and R_{ohmic} remain roughly constant at the original values of 0.47 V and 0.84 Ω-cm^2, respectively. While the Ag cathode performance seemingly improves at an ethanol concentration of 5 M, this effect is due to significant mass transport limitations at the anode (not shown), which improve the apparent performance at the other electrode. This behavior has been observed in other trials within our microfluidic fuel cell and may be due to the lack of fuel crossover under mass transport-limiting conditions [16].

3.3. *Effect of ethanol on a Cu triazole cathode*

Cu triazole, as a non-Pt catalyst, can be expected to yield inferior performance but greater ethanol tolerance. In addition, in our prior work we have seen that Cu triazole outperformed Ag on a mass activity basis [26]. However, the work to date on Cu triazole is fairly limited; here, we seek to test the activity of Cu triazole using our quantitative methodology as an example of a relatively new cathode catalyst. To test the ethanol tolerance of a Cu triazole cathode, the fuel cell was supplied with a 1 M KOH electrolyte containing varying concentrations of ethanol following the same procedure as used for the Pt electrode. Fig. 3b demonstrates that ethanol concentrations of up to 0.1 M have a negligible effect on Cu triazole, illustrating that Cu triazole is more tolerant of ethanol than Pt. An ethanol concentration of 0.5 M causes a 9% increase in R_{ohmic} (Table 2), indicating a minor decrease in performance, while an ethanol concentration of 2 M also causes a 20 mV increase in $\eta_{kinetic}$ due to ethanol reacting at the Cu triazole cathode. An ethanol concentration of 5 M causes substantial increase in overpotential of the Cu triazole cathode, a trend that is qualitatively similar as observed for the Pt cathode when exposed to 0.5 M EtOH. Due to the different

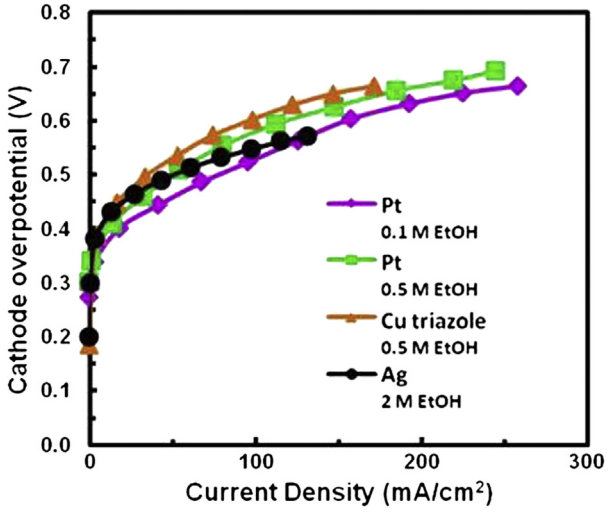

Fig. 4 – Cathode overpotential curve for varying ethanol concentrations and cathodes as a function of current density. Anode: Pt/C (1 mg Pt/cm^2); electrolyte: 1 M KOH; electrolyte flow rate: 0.6 ml/min; H_2/O_2 feeds: 10 SCCM. At room temperature.

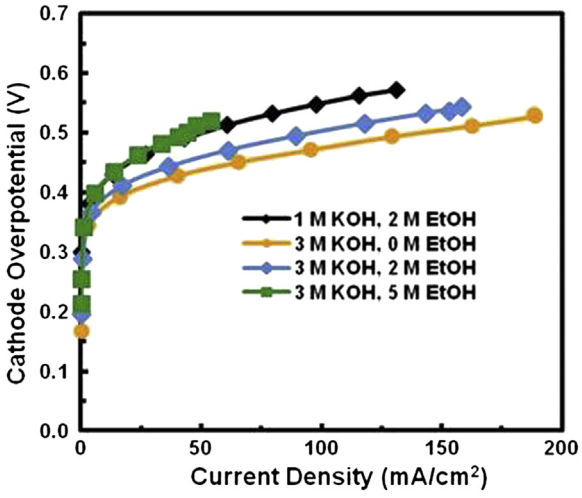

Fig. 5 – Cathode overpotential plot for varying ethanol concentrations and cathodes as a function of current density. Anode: Pt/C (1 mg Pt/cm^2); electrolyte flow rate: 0.6 ml/min; H_2/O_2 feeds: 10 SCCM. At room temperature.

Table 3 – Quantitative fits for Ag cathode with varying [EtOH] and [KOH].

[KOH] (M)	[EtOH] (M)	Cathode $\eta_{kinetic}$ (V)	Cathode R_{ohmic} (Ω cm^2)	Anode $\eta_{kinetic}$ (V)	Anode R_{ohmic} (Ω cm^2)
1	2	0.43	1.29	0.05	2.04
3	0	0.40	0.73	0.10	1.73
3	2	0.42	0.83	0.08	1.89

current range, the quantitative parameters from the Cu triazole trial cannot be compared to the other trials with Pt and Ag cathodes. While the Cu triazole electrode showed better tolerance to ethanol, the lower initial performance means that Cu triazole does not yield superior performance than a Pt cathode exposed to up to 0.5 M EtOH. However, the lower cost of Cu triazole makes it a viable choice for lower-cost fuel cell systems, possibly competing with Ag.

3.4. *Comparison of ethanol tolerance of the cathodes*

We also compared the ethanol tolerance of the three cathodes at varying ethanol concentrations using the data from the previous sections (Fig. 4). For Pt we used the data in the presence of 0.1 and 0.5 M ethanol, since the cathode exhibits a significant increase in overpotential in that range. For Cu triazole, the data obtained in the presence of 0.5 M EtOH was chosen. For Ag we took the data obtained in the presence of 2 M EtOH due to its constant performance between 0 and 2 M EtOH. Pt outperforms all other tested cathodes at ethanol concentrations $\leq$ 0.1 M, due to the superior initial performance. However, at ethanol concentrations of 0.5 M or higher, Ag outperforms Pt due to the mixed potential losses at the Pt cathode. In applications where a high level of ethanol crossover is expected, the selectivity of Ag makes it a superior catalyst. Cu triazole yielded inferior performance to the other two catalysts for the range of ethanol concentrations tested. While Cu triazole in its current form may outperform Pt at very high ethanol concentrations, Ag remains the superior alternative in those ranges and was used for the remainder of these cathode studies. Although the loading of Ag was higher than the loading of the other catalysts, this amount of Ag has a significantly lower cost than the other catalysts. The catalyst loading is also not expected to have a major effect relative to contaminant concentrations, as the contaminants are continuously flowed through the cell in large excess. These results demonstrate how different catalysts and their tolerance for ethanol can be compared quantitatively within a fuel cell using this methodology.

3.5. *Effect of pH on Ag ethanol tolerance*

The ethanol tolerance of the Ag cathode was investigated in the presence of 1 M KOH, which roughly corresponds to the OH^- concentration found in commercial membranes, and 3 M KOH, which is a higher concentration at times used in liquid electrolyte cells. Fig. 5 shows that the performance of the Ag cathode is superior in the presence of 3 M KOH. However, the tolerance to 2 M ethanol (see above) decreases when using the 3 M KOH electrolyte, as $\eta_{kinetic}$ increases from 0.40 V to 0.42 V and R_{ohmic} increases from 0.73 to 0.83 $\Omega \cdot cm^2$ (Table 3). While the increase in R_{ohmic} is largely due to the decreased conductivity in the presence of a higher EtOH concentration, the increase in $\eta_{kinetic}$ indicates that some ethanol is adsorbing and/or reacting at the cathode, which reduces the fuel efficiency. When comparing the cathode in the presence of 5 M and 0 M ethanol, $\eta_{kinetic}$ is roughly identical for both cases, but R_{ohmic} is approximately 240% larger than the value found in the absence of ethanol, possibly due to ethanol adsorption onto the cathode. Although operation with 3 M KOH yields slightly lower overpotentials than 1 M KOH (0.03 V lower value of $\eta_{kinetic}$), the lower fuel utilization at 3 M KOH, due to consumption of the fuel that crosses over, makes the optimal KOH concentration dependent on the particular application. In terms of power density, a 0.03 V decrease in $\eta_{kinetic}$ would roughly correspond to an 8% increase in power density for a cell operated at 0.4 V. Overall, an increase in pH may lead to a decrease in ethanol tolerance even for a highly tolerant Ag cathode, as additional hydroxyls facilitate ethanol oxidation.

3.6. *Effect of oxygen supply on ethanol tolerance of Ag cathodes*

To determine if convected oxygen improves ethanol tolerance of Ag cathodes, the microfluidic fuel cell operated with an air-breathing cathode exposed to quiescent air. Feeding a fuel cell with air, as opposed to oxygen from a tank, improves system energy density by eliminating the storage volume required for the tank, making the fuel cell more suitable for portable applications. Fig. 6 shows that supplying the Ag cathode with quiescent air, as opposed to convected oxygen, yields inferior

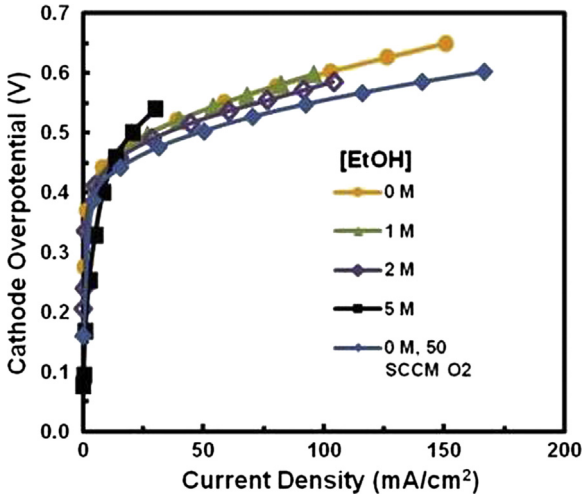

Fig. 6 – Cathode overpotential plot for varying ethanol concentrations as a function of current density for a Ag cathode. Anode: Pt/C (1 mg Pt/cm^2); cathode: Ag/C (4 mg Ag/cm^2); electrolyte: 1 M KOH; electrolyte flow rate: 0.6 ml/min; H_2/O_2 feeds: 10 SCCM. At room temperature.

Table 4 – Quantitative fits for Ag cathode with varying [EtOH] and [KOH].

Trial	Cathode $\eta_{kinetic}$ (V)	Cathode R_{ohmic} (Ω cm^2)	Anode $\eta_{kinetic}$ (V)	Anode R_{ohmic} (Ω cm^2)
0 M EtOH	0.47	1.11	0.03	2.20
1 M EtOH	0.47	1.30	0.08	2.43
2 M EtOH	0.45	1.48	0.10	2.62
0 M EtOH, 50 SCCM O_2	0.47	0.78	0.06	2.04

performance. Specifically, $\eta_{kinetic}$ is 13 mV greater, as would be expected from the reduced oxygen concentration, and R_{ohmic} increases by 43%, due to the lack of convection and reduced oxygen supply (Table 4). However, the air-breathing Ag cathode still shows high tolerance to ethanol concentrations of up to 2 M (Fig. 6). An ethanol concentration of 5 M did cause performance degradation when operating the cell with quiescent air, whereas the performance did not drop when operating the cell with the convected oxygen. This decreased tolerance is likely caused by the lower oxygen concentration in air and would be expected to hold for other catalysts, such as Cu triazole. The decrease in performance at 5 M EtOH with quiescent air, as opposed to convected O_2, also follows the previously established trend that a higher ethanol to oxygen ratio reduces system ethanol tolerance.

3.7. *Effect of oxygen supply on ethanol tolerance of Pt cathodes*

Based on the preceding result, the microfluidic fuel cell was operated with varying oxygen concentrations to determine whether the ethanol tolerance of a Pt cathode was dependent on the oxygen supply. Air is well-known to reduce fuel cell power density due to its lower oxygen concentration relative to pure oxygen [5]. However, the dependence of contaminant tolerance on air supply has not been studied extensively. To investigate this effect and to determine the importance of the ethanol to oxygen molar ratio, the fuel cell was tested with oxygen fractions of 21, 41, and 75 mol % in the cathode feed by altering the relative amounts of oxygen and nitrogen. Fig. 7a shows the losses for the cathode as a function of oxygen concentration: the 21% oxygen (air) feed exhibits a $\eta_{kinetic}$ of 330 mV, 30 mV greater than the value of 300 mV for the 75% oxygen feed, with the 41% oxygen feed performing similarly to the 75% oxygen feed. When 2 M EtOH is added to the electrolyte, the cathode performs worse, as expected, for all three oxygen concentrations, with increased losses in $\eta_{kinetic}$ of 0.11 V for the 21% oxygen and 75% oxygen feeds and increases in R_{ohmic} of 54% and 41%, respectively. However, the performance of the 41% oxygen feed drops more than the other two feeds, ending up at the same value of $V_{kinetic}$ as the 21% oxygen feed and having an increased value of R_{ohmic} of 71% over the value with no ethanol present. This result indicates the importance of oxygen supply; operation in the presence of a lower oxygen concentration leaves the system more vulnerable to contamination, so even double the concentration found in air does not result in improved performance if sufficient ethanol contamination is present to react with the oxygen.

3.8. *Effect of acetic acid on Pt electrode performance*

Acetic acid, as a common undesired product of ethanol oxidation, may be present in the electrolyte, where it reacts with KOH to yield potassium acetate and water. This problem may be particularly pronounced when using a Pt cathode, since Pt produces large amounts of acetic acid when ethanol crosses over from the anode side of the cell [4]. To study the effect of acetic acid contamination, the microfluidic cell was operated with varying amounts of acetic acid added to a 1 M

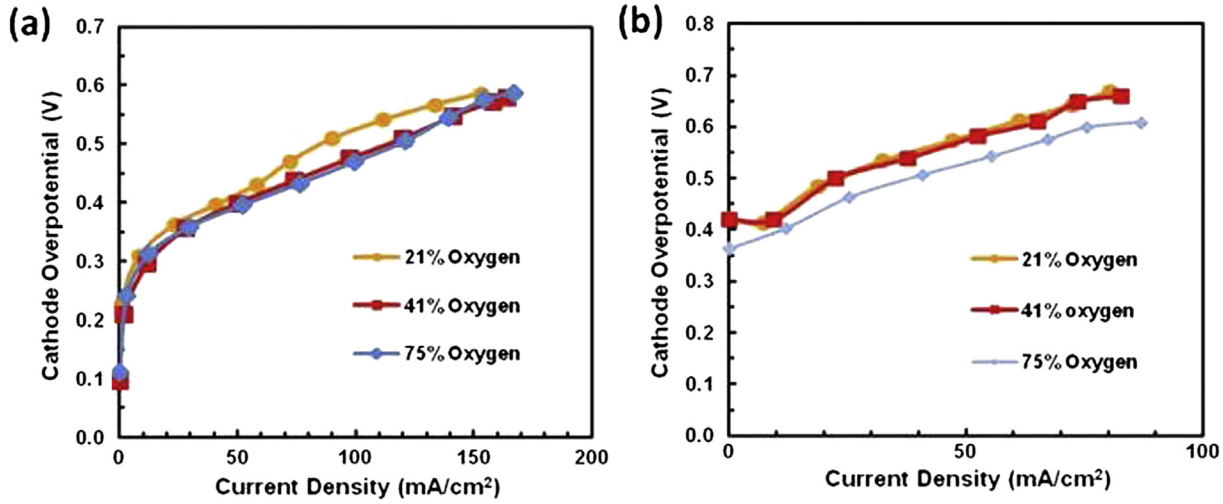

Fig. 7 – Cathode overpotential plot for varying oxygen concentrations as a function of current density for a Pt cathode with (a) 0 M EtOH and (b) 2 M EtOH in the electrolyte. Anode: Pt/C (1 mg Pt/cm^2); cathode: Ag/C (4 mg Ag/cm^2); electrolyte: 1 M KOH; electrolyte flow rate: 0.6 ml/min; H_2/cathode feeds: 20 SCCM. At room temperature.

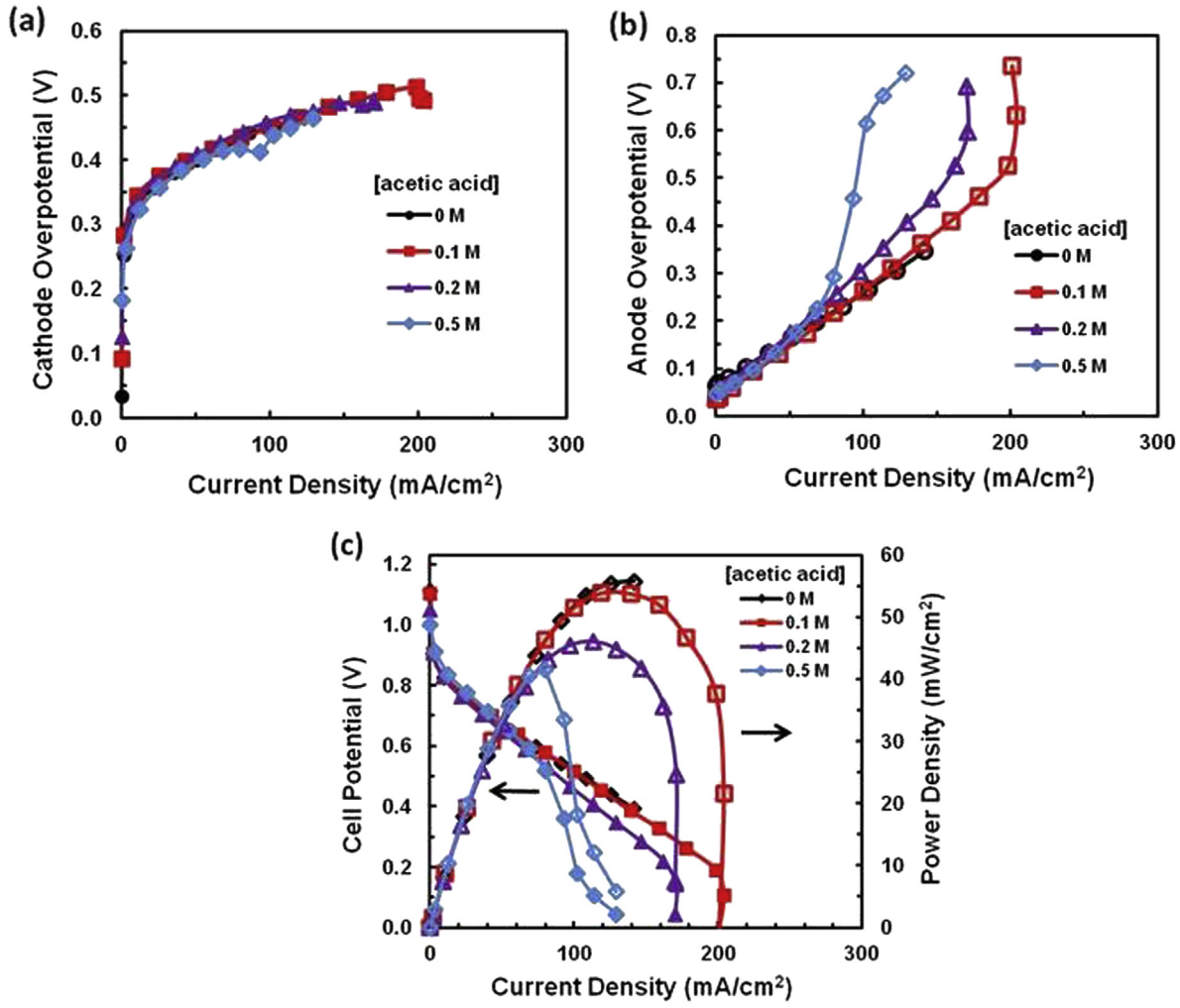

Fig. 8 – Single electrode plots for (a) the cathode and (b) the anode and (c) olarization and power density curves for varying acetic acid concentrations as a function of current density. Anode: Pt/C (1 mg Pt/cm^2); cathode: Pt/C (1 mg Pt/cm^2); electrolyte: 1 M KOH; electrolyte flow rate: 0.6 ml/min; H_2/O_2 feeds: 10 SCCM. At room temperature.

KOH electrolyte. Fig. 8a shows that the addition of acetic acid up to 0.5 M does not significantly affect cathode performance. The oddly low point near 100 mA/cm^2 aligns with an inflection point for the anode (Fig. 8b); this type of inflection may indicate a decrease in the local anode pH. Since the anode is consuming hydroxyls, the pH may decrease at higher current densities, resulting in unstable performance until a very high overpotential attracts more hydroxyls from further away in the electrolyte. This type of mass transport limitation is the cause of the inferior anode performance in the presence of 0.2 and 0.5 M acetic acid. Quantitatively, while the cathode performances do not significantly differ, the R_{ohmic} of the anode increased by 25% when the acetic acid concentration increased from 0.1 M to 0.2 M, showing that the reduced hydroxyl supply interferes with anode performance (Table 5). The limitations from the hydroxyl supply are minor until higher current densities are reached, so the anode performance is similar at lower current densities, independent of the acetic acid concentration.

The power density curves in Fig. 8c show a significant decrease in performance for cells operated in the presence of acetic acid concentrations ≥0.2 M. The power density drops by 17% and 26%, respectively, in the presence of 0.2 and 0.5 M acetic acid. The difference in performance between the

Table 5 – Quantitative fits for Pt electrodes with varying acetic acid.

[Acetic acid] (M)	Cathode $\eta_{kinetic}$ (V)	Cathode R_{ohmic} (Ω•cm^2)	Anode $\eta_{kinetic}$ (V)	Anode R_{ohmic} (Ω•cm^2)
0	0.35	1.67	0.06	1.34
0.1	0.37	0.82	0.02	2.41
0.2	0.37	0.80	0.02	2.99
0.5	0.36	0.82	–	–

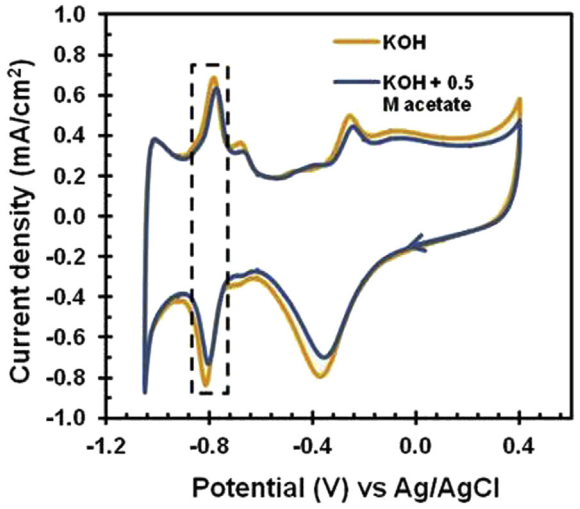

Fig. 9 – Cyclic voltammograms of a 20 wt% Pt/C RRDE in the presence of 1 M KOH or 1 M KOH with 0.5 M acetic acid. Scan rate: 50 mV/s. At room temperature under Ar.

Table 6 – Quantitative fits for Pt anode with varying [EtOH].

[EtOH] (M)	Anode $\eta_{kinetic}$ (V)	Anode R_{ohmic} (Ω cm^2)
0	0.03	2.38
0.5	0.04	2.40
2	0.05	2.40
5	0.07	3.73

experiments performed with various acetic acid concentrations is small at current densities below 70 mA/cm^2, which indicates that the hydroxyl supply is sufficient at these concentrations. Carbonate formation, where the CO_2 formed from complete ethanol oxidation forms carbonate anions from the hydroxyls in the electrolyte, may have a similar effect. A similar pattern of a relatively small initial drop in power density followed by sharper decreases, with increasing carbonate content, was evident in our previous work analyzing carbonate contamination [7,16]. Whether ethanol oxidizes partially or fully at the anode, oxidized ethanol will still inhibit fuel cell performance if left unchecked over time.

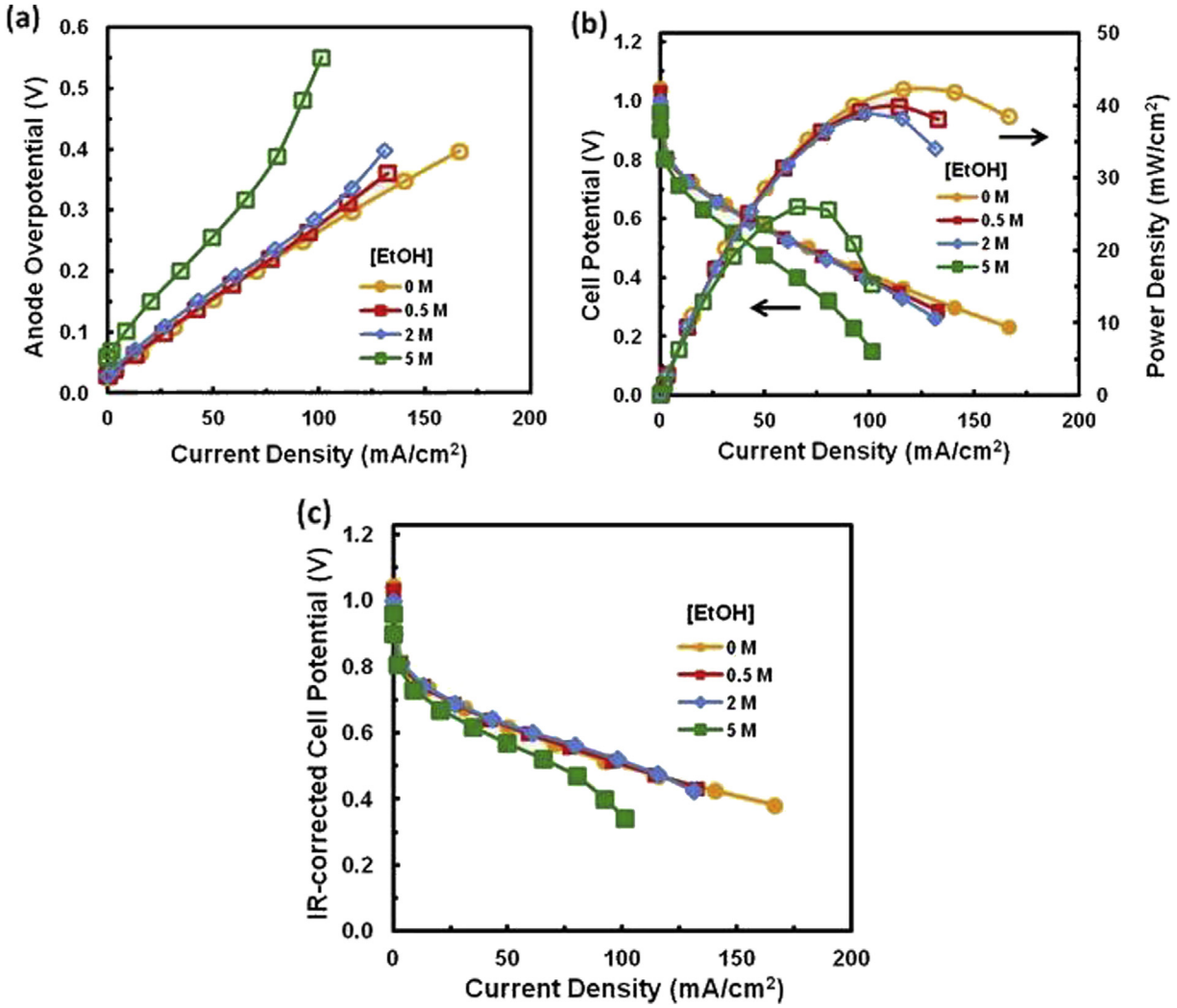

Fig. 10 – Single electrode curves for (a) the anode, (b) polarization and power density curves, and (c) IR-corrected polarization curves for varying ethanol concentrations as a function of current density. Anode: Pt/C (1 mg Pt/cm^2); cathode: Pt/C (1 mg Pt/cm^2); electrolyte: 1 M KOH; electrolyte flow rate: 0.6 ml/min; H_2/O_2 feeds: 10 SCCM. At room temperature.

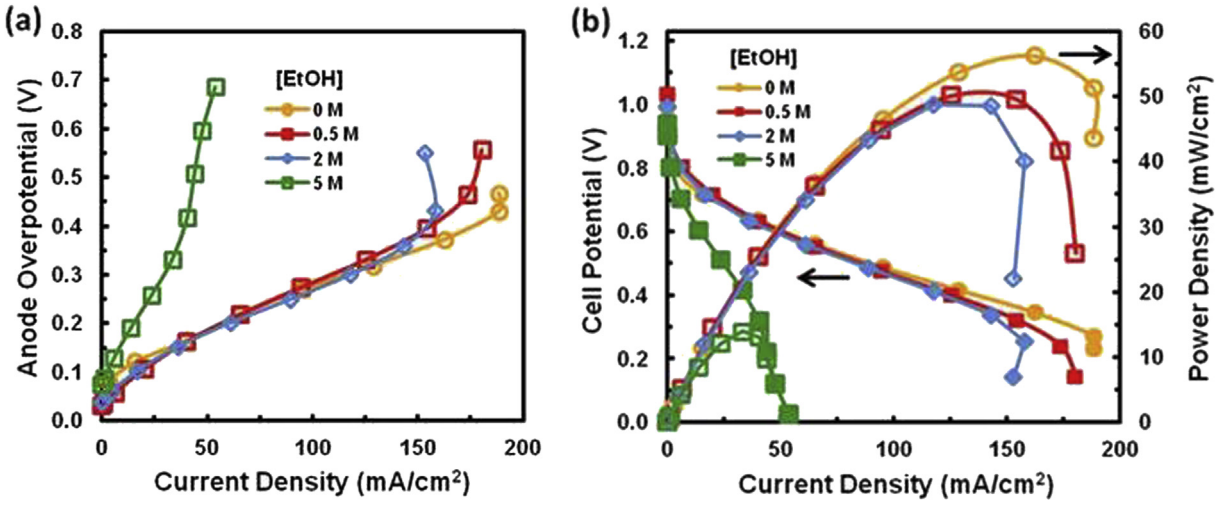

Fig. 11 – Single electrode plot for (a) the anode and (b) polarization and power density curves, s for varying ethanol concentrations as a function of current density. Anode: Pt/C (1 mg Pt/cm^2); cathode: Pt/C (1 mg Pt/cm^2); electrolyte: 3 M KOH; electrolyte flow rate: 0.6 ml/min; H_2/O_2 feeds: 10 SCCM. At room temperature.

To determine whether the observed performance degradation is due to adsorption of acetic acid onto the Pt catalyst, a Pt/C coated rotating ring disk electrode (RRDE) was tested under alkaline conditions using a 1 M KOH electrolyte. A cyclic voltammogram (CV) (Fig. 9) was used to identify the electrochemically active surface area of the Pt/C catalyst in the presence and absence of acetate. The area under the peak centered around −0.8 V vs Ag/AgCl corresponds to hydrogen desorption in alkaline media, which correlates with the electrochemically active surface area (ECASA) [35]. The CV shows that the electrochemically active surface area slightly decreases in the presence of acetic acid, but this amount of lost surface area is not sufficient to explain the 26% performance decrease (Fig. 8c). Therefore, we conclude that the lower pH is the main cause for lower performance at higher concentrations of acetic acid.

Acetaldehyde is another contaminant species that can be produced in significant amounts and thus relevant to fuel cell operation. While acetaldehyde may play a significant role, we here focused on catalyst studies with respect to longer term operation. Once formed, acetaldehyde can be oxidized to the terminal products of acetic acid and CO_2, so the study of those two products and the fuel itself assumes greater importance [10]. Although the direct effect of acetaldehyde is not studied here, this effect would be important for future studies.

3.9. *Effect of ethanol on Pt electrode performance*

Ethanol can be present at the anode in a hydrogen fuel cell due to incomplete fuel reforming of ethanol to produce the hydrogen feed or due to environmental contamination. Ethanol at the anode does not cause the same crossover problems as ethanol at the cathode, but ethanol oxidation can still compete with the desired hydrogen oxidation reaction. The fuel cell was tested with a Pt anode and a Ag cathode with varying amounts of ethanol added to the 1 M KOH electrolyte. The Ag cathode was chosen due to its ethanol tolerance. Fig. 10 shows that the effect of ethanol is minor up to 2 M, with only a slight decrease in performance along with slightly earlier onset of mass transport limitations. The IR-corrected polarization curves in Fig. 10c are not substantially different from the corresponding uncorrected polarization curves, demonstrating that the performance loss is not caused by the slight decrease in conductivity due to the presence of ethanol. In contrast, the presence of ethanol at a concentration of 5 M causes a substantial decrease in anode performance and an overall decrease in power density of 32%. $\eta_{kinetic}$ increases by 40 mV and R_{ohmic} increases by 57% (Table 6), indicating significant kinetic losses that are in this case due to competing ethanol oxidation occurring on the same electrode. However, this performance loss occurs at ethanol concentrations that

Table 7 – Quantitative fits for Pt anode with varying [EtOH].

[EtOH] (M)	Cathode $\eta_{kinetic}$ (V)	Cathode R_{ohmic} (Ω cm^2)	Anode $\eta_{kinetic}$ (V)	Anode R_{ohmic} (Ω cm^2)
0	0.40	0.73	0.10	1.73
0.5	0.41	0.74	0.09	1.98
2	0.42	0.83	0.08	1.89
5	0.40	2.44	0.09	7.16

would not likely be encountered as a contaminant in a fuel cell. Other possible anode catalysts such as Ni, which is less active for ethanol oxidation, would thus be expected to have ethanol tolerance levels as high as Pt when used as the anode in a H_2 fuel cell.

The same experiment was also conducted in the presence of 3 M KOH. Fig. 11a shows a similar trend for 3 M KOH as for 1 M KOH, with ethanol concentrations $\leq$2 M having a minimal impact. However, the effect of ethanol at 5 M is much more pronounced in the presence of 3 M KOH, causing a 75% drop in power density. The anode performance is also far worse, with a very large increase in R_{ohmic} of 310% (Table 7). This level of degradation shows that ethanol oxidation is beginning to dominate over the hydrogen oxidation. The likely cause of this behavior is the increased amount of acetate at higher pH, which will adsorb more readily onto the electrodes in alkaline conditions.

4. Conclusions

Here, we quantified the effect of ethanol contamination on electrode performance in a microfluidic fuel cell using single electrode plots. Ethanol contamination can cause problems at both the cathode and the anode for Pt electrodes in alkaline media. Ag is insensitive to ethanol up to 2 M and can outperform Pt when local ethanol concentrations are at 0.5 M or higher, demonstrating that silver is the optimal catalyst of those tested when substantial ethanol crossover occurs. Using the same method, Cu triazole exhibits more ethanol tolerance than Pt and less ethanol tolerance than Ag, demonstrating that this method can be used to screen less studied cathode catalysts. We also demonstrated that the ethanol to oxygen molar ratio affects ethanol tolerance, and that RDE experiments performed in the presence of relatively low amounts of ethanol may display artificially low ethanol tolerance due to the low concentration of dissolved oxygen. At the anode, ethanol has only a minor impact on performance under ordinary fuel cell operating conditions. Furthermore, acetic acid contamination has a negligible effect on Pt cathodes but can significantly inhibit anode performance, due largely to the decrease in pH.

Quantitative analysis of the effects of ethanol (and acetic acid) contamination on electrode performance as reported in this paper will aid the development of optimal fuel cell design in which ethanol crossover can be a problem. The quantitative method can be used to screen novel cathode catalysts with the transport phenomena intrinsic to a fuel cell, phenomena that cannot easily be simulated in a RDE experiment. Each electrode can be selected based on the predicted ethanol concentration at the electrode, eliminating the need to test multiple fuel cell configurations under multiple operation conditions. These results also demonstrate that a cathode catalyst may show lower contaminant tolerance when tested with a lower oxygen concentration. Proper cathode selection can also enable the use of higher ethanol concentrations than would be optimal when using a Pt cathode, improving system energy density for portable applications. Tests similar to the ones reported in this paper, but, for example, at higher current density and higher temperature, can be performed to directly link performance with operation conditions in fuel cells intended for commercial application. Similarly, long-term experiments to examine electrode stability in the presence of ethanol, acetic acid, as well as the acetaldehyde, can be performed to improve understanding of ethanol contamination in alkaline fuel cells.

Acknowledgments

We gratefully acknowledge financial support from the Department of Energy (DE-FG02005ER46260) and from the Dow Chemical Company for a graduate fellowship to MSN.

REFERENCES

[1] Li YS, Zhao TS, Liang ZX. Performance of alkaline electrolyte-membrane-based direct ethanol fuel cells. Journal of Power Sources 2009;187:387–92.
[2] Lee E, Murthy A, Manthiram A. Effect of Mo addition on the electrocatalytic activity of Pt-Sn-Mo/C for direct ethanol fuel cells. Electrochimica Acta 2011;56:1611–8.
[3] Demirci UB. Direct liquid-feed fuel cells: thermodynamic and environmental concerns. Journal of Power Sources 2007;169:239–46.
[4] Li G, Pickup PG. Analysis of performance losses of direct ethanol fuel cells with the aid of a reference electrode. Journal of Power Sources 2006;161:256–63.
[5] Carrette L, Friedrich KA, Stimming U. Fuel cells: principles, types, fuels, and applications. Chemphyschem 2000;1:162–93.
[6] Gülzow E. Alkaline fuel cells. Fuel Cells 2004;4:251–5.
[7] Naughton MS, Brushett FR, Kenis PJA. Carbonate resilience of flowing electrolyte-based alkaline fuel cells. Journal of Power Sources 2011;196:1762–8.
[8] Tarasevich M, Bogdanovskaya V, Mazin P. Electrocatalysts and membrane for direct ethanol-oxygen fuel cell with alkaline electrolyte. Russian Journal of Electrochemistry 2010;46:542–51.
[9] Li YS, Zhao TS, Chen R. Cathode flooding behaviour in alkaline direct ethanol fuel cells. Journal of Power Sources 2010;196:133–9.
[10] Melke J, Schoekel A, Dixon D, Cremers C, Ramaker DE, Roth C. Ethanol oxidation on carbon-supported Pt, PtRu, and PtSn catalysts studied by operando X-ray absorption spectroscopy. The Journal of Physical Chemistry C 2010;114:5914–25.
[11] Antolini E, Gonzalez ER. Alkaline direct alcohol fuel cells. Journal of Power Sources 2010;195:3431–50.
[12] Antolini E. Catalysts for direct ethanol fuel cells. Journal of Power Sources 2007;170:1–12.
[13] Shen SY, Zhao TS, Wu QX. Product analysis of the ethanol oxidation reaction on palladium-based catalysts in an anion-exchange membrane fuel cell environment. International Journal of Hydrogen Energy 2012;37:575–82.
[14] Mann J, Yao N, Bocarsly AB. Characterization and analysis of new catalysts for a direct ethanol fuel cell. Langmuir 2006;22:10432–6.
[15] James DD, Bennett DV, Li G, Ghumman A, Helleur RJ, Pickup PG. Online analysis of products from a direct ethanol fuel cell. Electrochemistry Communications 2009;11:1877–80.
[16] Brushett FR, Naughton MS, Ng JWD, Yin L, Kenis PJA. Analysis of Pt/C electrode performance in a flowing-

electrolyte alkaline fuel cell. International Journal of Hydrogen Energy 2011;37:2559–70.
[17] Jiang L, Hsu A, Chu D, Chen R. Oxygen reduction reaction on carbon supported Pt and Pd in alkaline solutions. Journal of the Electrochemical Society 2009;156:B370–6.
[18] Crc Handbook of Chemistry and Physics. Boca Raton, FL: CRC Press/Taylor; 2009.
[19] Haryanto A, Fernando S, Murali N, Adhikari S. Current status of hydrogen production techniques by steam reforming of ethanol: a review. Energy & Fuels 2005;19:2098–106.
[20] Wang W, Wang Y, Liu Y. Production of hydrogen by ethanol steam reforming over nickel–metal oxide catalysts prepared via urea–nitrate combustion method. International Journal of Energy Research 2010;35:501–6.
[21] Zhang B, Tang X, Li Y, Xu Y, Shen W. Hydrogen production from steam reforming of ethanol and glycerol over ceria-supported metal catalysts. International Journal of Hydrogen Energy 2007;32:2367–73.
[22] Vasudeva K, Mitra N, Umasankar P, Dhingra SC. Steam reforming of ethanol for hydrogen production: thermodynamic analysis. International Journal of Hydrogen Energy 1996;21:13–8.
[23] Brushett FR, Zhou WP, Jayashree RS, Kenis PJA. Alkaline microfluidic hydrogen-oxygen fuel cell as a cathode characterization platform. Journal of the Electrochemical Society 2009;156:B565–71.
[24] Jayashree RS, Mitchell M, Natarajan D, Markoski LJ, Kenis PJA. Microfluidic hydrogen fuel cell with a liquid electrolyte. Langmuir 2007;23:6871–4.
[25] Brushett FR, Duong HT, Ng JWD, Behrens RL, Wieckowski A, Kenis PJA. Investigation of Pt, Pt3Co, and Pt3Co/Mo cathodes for the ORR in a microfluidic H-2/O-2 fuel cell. Journal of the Electrochemical Society 2010;157:B837–45.
[26] Brushett FR, Thorum MS, Lioutas NS, Naughton MS, Tornow C, Jhong HR, et al. A carbon-supported copper complex of 3,5-Diamino-1,2,4-triazole as a cathode catalyst for alkaline fuel cell applications. Journal of the American Chemical Society 2010;132:12185–7.
[27] Choban ER, Waszczuk P, Kenis PJA. Characterization of limiting factors in laminar flow-based membraneless microfuel cells. Electrochemical and Solid-state Letters 2005;8:A348–52.
[28] Naughton MS, Moradia AA, Kenis PJA. Quantitative analysis of single-electrode plots to understand in-situ behavior of individual electrodes. Journal of the Electrochemical Society 2012;159:B761–9.
[29] Thorum Matthew S, Yadav J, Gewirth Andrew A. Oxygen reduction activity of a copper complex of 3,5-Diamino-1,2,4-triazole supported on carbon black. Angewandte Chemie 2009;121:171–3.
[30] Gülzow E, Schulze M. Long-term operation of AFC electrodes with CO2 containing gases. Journal of Power Sources 2004;127:243–51.
[31] Spendelow JS, Wieckowski A. Electrocatalysis of oxygen reduction and small alcohol oxidation in alkaline media. Physical Chemistry Chemical Physics 2007;9:2654–75.
[32] Whipple DT, Jayashree RS, Egas D, Alonso-Vante N, Kenis PJA. Ruthenium cluster-like chalcogenide as a methanol tolerant cathode catalyst in air-breathing laminar flow fuel cells. Electrochimica Acta 2009;54:4384–8.
[33] Thorum MS, Hankett JM, Gewirth AA. Poisoning the oxygen reduction reaction on carbon-supported Fe and Cu electrocatalysts: evidence for metal-centered activity. The Journal of Physical Chemistry Letters 2011;2:295–8.
[34] Jhong H-R, Brushett FR, Yin L, Stevenson DM, Kenis PJA. Combining structural and electrochemical analysis of electrodes using micro-computed tomography and a microfluidic fuel cell. Journal of the Electrochemical Society 2012;159:B292–8.
[35] Tammeveski K, Tenno T, Claret J, Ferrater C. Electrochemical reduction of oxygen on thin-film Pt electrodes in 0.1 M KOH. Electrochimica Acta 1997;42:893–7.